**Title**
Engineering antibiotic loaded gelatin methacryloyl based nanoparticles for sustained drug delivery



**Author**
Liu, Yangcheng

**Publication Date**
2021

Peer reviewed|Thesis/dissertation

UNIVERSITY OF CALIFORNIA

Los Angeles

# Engineering antibiotic loaded gelatin methacryloyl based nanoparticles for sustained drug delivery

A thesis submitted in partial satisfaction

of the requirements for the degree Master of Science

in Chemical Engineering

by

Yangcheng Liu

2021

ABSTRACT OF THE THESIS

Engineering antibiotic loaded gelatin methacryloyl based nanoparticles

for sustained drug delivery

by

Yangcheng Liu

Master of Science in Chemical Engineering

University of California, Los Angeles, 2021

Professor Nasim Annabi, Chair

Eye injuries and diseases remain as a challenging clinical issue to deal with worldwide. Due to the existence of ocular drug transport barriers, conventional administration methods have shown several limitations, such as low bioavailability and poor patient compliance. Therefore, we formulated gelatin methacryloyl (GelMA) based nanoparticles (NPs) which can be loaded with hydrophilic drug molecules such as antibiotics. These NPs can be incorporated into a hydrogel patch composed of GelMA and glycidyl methacrylated hyaluronic acid (HAGM) for sustained

drug release to treat the target site of bacterial infection in the eye. The engineered GelMA based NPs were characterized *in vitro* and demonstrated ideal hydrodynamic size (particle diameter: 221 ± 11 nm), homogeneity (PDI: 0.21 ± 0.02) and loading efficiency (93.8 ± 8.2%), facilitating drug penetration and bioavailability in the eye. The GelMA/HAGM hydrogel patch (GelPatch) was prepared by dissolving the polymers and photoinitiators in an aqueous solution and photo-crosslinked for 4 min under visible light (450 to 550 nm). The *in vitro* release profiles of moxifloxacin (MXF) loaded GelMA NPs incorporated inside GelPatch were studied. An initial quick release was followed by a sustained release of 70% of loaded MXF for 5 days. Such release profile is desirable for treating eye infection because the initial 30% of released MXF can kill bacteria and the therapeutic effect can be retained for several days. Incorporation of GelMA NPs also enhanced the physical properties of GelPatch, in terms of adhesion (burst pressure: 40.8 ± 4.2 kPa), which has surpassed the eye pressure ranges (2.7 to 4.0 kPa) of patients with eye diseases, and elasticity (compressive modulus: 40.47 ± 2.7 kPa, tensile modulus: 42.754 ± 2.03 kPa). The biocompatibility of GelPatch containing NPs was confirmed *in vitro* by providing > 90% cell viability. In addition, the MXF loaded NPs were highly effective against both gram-positive (*Pseudomonas aeruginosa*) and gram-negative (*Staphylococcus aureus*) bacteria based on the results from zone of inhibition (diameter: 28 to 30 mm) as well as the colony forming assay. With the advantages of easy formulation and application, good biocompatibility, and promising antimicrobial function, the GelMA NPs loaded in GelPatch, possess the potential for further application in treating ocular diseases in a safe, effective and patient compliant way.

The thesis of Yangcheng Liu is approved.

Panagiotis D. Christofides

Yunfeng Lu

Nasim Annabi, Committee Chair

University of California, Los Angeles

2021

**Table of Contents**

**List of Figures**

**Acknowledgements**

If it was not for the people who I had met and people I had lost during my life, I would not be who I am today and accomplish any achievements.

I would like to thank my parents, Jun Gao and Sande Liu for bringing me to this wonderful world. Nothing would have been possible without their selfless support and continuous encouragement. Benefited from my parent's envisioning, integrity and tenacity, I have always been feeling fearless to face and to overcome any challenges in my life.

Thanks to Dr. Shrinivasa K. Dr. Upadhyaya, Dr. D. Ken Giles and many other faculty members who I have worked with in UC Davis during my undergraduate studies for sharing their creative thoughts and guiding me to step forwards on the path of scientific research.

Thanks to Dr. Nasim Annabi, for accepting me as a Master's student. I am grateful for all the opportunities and advice you provided with me to learn and to grow as a scientific researcher.

Thanks to Ann Yung, Dr. Reza Dana and Dr. Paulo Bispo for the valuable collaboration.

Thanks to every fellow lab member. Thank you Dr. Shima Gholizadeh for teaching me research skills.

In the end, I would also like to thank my grandmother, who passed away two years ago due to MODS. Your sudden leaving made up my mind to contribute more on pharmaceutical research and your belief in the power of education will guide me to continuously improve myself as a person.

## Chapter 1. Background and Introduction

There is an increase in the prevalence of eye diseases such as glaucoma, dry eye disease and age-related macular degeneration. This is mainly correlated with the increase of an aging population, changes in lifestyle and prolonged wear of contact lenses worldwide [1-3]. Apart from chronic disease-based eye injuries, acute physical injuries, spanning from superficial abrasions to full-thickness perforations, can result from a variety of causes including blunt force injuries, penetration of foreign bodies, and chemical burns, among others.

In general, ocular induced primary injuries due to either chronic disease or physical abrasions are associated with a high risk of infection due to breakdown and/or rupture of the main barrier (i.e., surface epithelium layer) on the cornea or sclera which may permit infiltration of microorganism into the eye [4]. Bacterial infection is one of the main causes of many eye-related inflammations which can lead to conjunctivitis, keratitis and endophthalmitis, and thus need antibiotic-based therapeutic intervention.

Bacterial keratitis is caused by bacterial (e.g., *Pseudomonas aeruginosa* and *Staphylococcus aureus*) infection in the cornea, which refers to the arc shaped layer covering the colored portion of eyes [5]. Conjunctivitis, which is a more common eye disease, is as a result of inflammation of a thin semi-transparent membrane on the inner surface of eyelids due to the bacterial infection [6]. With timely treatment, most of these diseases can be treated in less than two weeks. However, nearly 6 million people were affected by acute conjunctivitis in the United States each year [6].

An average of $ 617 million was spent on the treatment of bacterial conjunctivitis annually by U.S. medical institutions [7].

Topical ophthalmic antibiotics are the most commonly used drug administration route via topical instillation. It is often applied to relieve the inflammation symptoms and facilitate recovering process. In specific cases such as endophthalmitis (i.e., serious inflammation of the interior of eyes), the common methodology is based on direct injection of antibiotics to the eye through a specialized needle [8]. The topical instillation has a poor bioavailability, because of mechanisms such as reflex blinking and tear-film turnover [9]. Due to the presence of static and dynamic ocular barriers, less than 5% of a dose can be delivered to the posterior segment of eyes [10-11]. To overcome these challenges, researchers have developed various ocular drug delivery methods such as periocular and intravitreal injection, oral and subconjunctival administration. Unlike topical instillation, intravitreal injection can be used to apply drugs directly in the affected area in the eye, achieving better therapeutic effect. However, it is not patient compliant and can cause serious side effects including hemorrhage and retinal detachments. Oral route, on the other hand, is noninvasive. But, since high dosage is required to achieve equivalent therapeutic effect, it can cause toxicity and side effects [12]. For example, doxycycline is used as an anti-inflammatory drug in eye disease treatment. However, it can induce gastrointestinal upset and harm immature livers and kidneys. Furthermore, it is challenging to achieve sustained release in either intravitreal injection or systematic administration due to the burst release of drug with short effective duration and consequently high frequency of therapeutic application [13]. Thus, an efficient and noninvasive ocular drug delivery system with sustained release is still an unmet clinical need, specifically for chronic ocular inflammation conditions.

With the spread of Covid-19, people rely even more heavily on smart medicine or devices to be applied as next generation therapeutics. So far, NPs, applied either in a form of suspension or embedded inside a solid matrix (i.e., devices), have shown promising outcomes for drug delivery purposes [14]. The NP-based drug delivery systems can be composed of self-assembled proteins or peptides, synthetic block co-polymers, or lipids [15-16]. Natural polymer-based NPs have several advantages over synthetic polymers such as high biocompatibility, non-toxic byproducts, and low cost of production. Among the natural polymers, gelatin, a denatured form of collagen, is a versatile class of naturally occurring biopolymers. Gelatin is a proteinaceous linear polymer obtained by the partial hydrolysis (acidic or basic) of collagen. Depending on the process used, gelatin is produced as type-A or type-B gelatin. While the acidic treatment yields type-A gelatin, with an isoelectric point at around 9 and a broad molecular weight profile, the alkaline hydrolysis yields type-B gelatin, with an isoelectric point at around 5 [17].

Gelatin has been exploited as a drug carrier system owing to its chemical and physical nature. The influence of pH and temperature on the phase behavior of gelatin in solution makes it an interesting candidate for drug delivery applications. The abundant functional groups on gelatin backbone offer the advantage of incorporating functionalities, conjugating different drugs, or modifying it with synthetic polymers such as polyethylene glycol (PEG) [18]. So far, gelatin-DNA complexation in the form of nanospheres as gene delivery vehicles have been reported [19]. Gelatin-coated magnetic iron oxide NPs have been also synthesized and evaluated its potential to serve as a drug carrier system for magnetic drug targeting, used in cancer treatment [20]. Moreover, combination

of GelMA with chitosan has been applied in formulating NPs loaded with a growth factor peptide for building pre-vascularized tissue and sealing wounds [21]. However, none of these NPs are designed specifically for ocular drug delivery and suffer from large particle sizes (> 300 nm) as well as low encapsulation efficiency (< 60%). Besides, sustained release effect was not achieved in any of these NP-based delivery systems.

To overcome these limitations, in this thesis, an ocular nano-delivery platform composed of GelMA NPs was designed in order to achieve a sustained antibiotic release profile for the treatment of infected eyes. These GelMA based NPs were loaded with MXF which is a highly potent antibiotic from class of antibiotics called fluoroquinolones. MXF is a broad-spectrum antibiotic, effective towards both gram-positive and gram-negative bacteria [22]. In order to improve the ocular retention of NPs, a hydrogel matrix, GelPatch, was also synthesized, which can be loaded with NPs at a desired drug concentration to reach a long term sustained drug release profile. The GelPatch is a photocrosslinked hydrogel network based on GelMA and HAGM which is highly adhesive to the corneal tissue with minimized swelling properties and certain porosity to maximize drug delivery across the gel via diffusion.

To form GelPatch loaded with NPs containing MXF, we first developed and optimized MXF loaded GelMA NPs. The NP formulations were characterized for their size, polydispersity index (PDI), and encapsulation efficiency of MXF. *In vitro* release studies were performed to check the release profile of the developed NPs. At the second step, the optimized MXF loaded NP formulation was incorporated into an adhesive hydrogel, GelPatch which is a visible light

crosslinkable drug delivery platform (applicable to the sclera surface). The NPs loaded GelPatch was further characterized for drug release, mechanical strength, swelling and adhesion. Finally, the *in vitro* cell studies and antibacterial tests were carried out to check the biocompatibility, and antimicrobial effect of our developed nanoscale drug delivery platform, respectively.

## Chapter 2. Materials and Methods

### 2.1 Materials

Gelatin from porcine skin (Bloom 300, type A), methacrylic anhydride 94%, Eosin Y, triethanolamine (TEA) and N-vinylcaprolactam 98% (VC) were all purchased from Sigma-Aldrich. Hyaluronic acid (HA) sodium salt from Streptococcus equi (Mw: 1.6 MDa) was purchased form Sigma-Aldrich. MXF hydrochloride was obtained from 1Click Chem. Dulbecco's phosphate buffered saline (DPBS) was purchased from GE Healthcare Life Sciences. Other chemicals and organic solvents used in this study were purchased from Sigma-Aldrich and used as received, unless stated otherwise.

### 2.2 Synthesis of GelMA

GelMA was synthesized based on the procedures explained before [23]. Briefly, 10% (w/v) of gelatin was dissolved in DPBS solution and reacted with 8% (v/v) of methacrylic anhydride at 60℃ for 4 hr. After the methacrylate reaction stopped, the solution was then filled in dialysis membranes and dialyzed for 5 days to remove excess methacrylic anhydride remained. The solution was then transferred into falcon tubes and freeze-dried at -80℃ for 5 days.

### 2.3 Synthesis of HAGM

HAGM was synthesized using a previously described protocol [24]. Briefly, 10% (v/w) of HA sodium salt (1.6 MDa, Sigma-Aldrich) was dissolved in 200 mL of deionized (DI) water for 12 hr under vigorous stirring. Once dissolved, 8 mL of triethylamine (Sigma-Aldrich), 8 mL of glycidyl

methacrylate (Sigma-Aldrich), and 4 g of tetrabutyl ammonium bromide (TBAB) (Sigma-Aldrich) were added separately in the mentioned order and allowed to fully mix for 1 hr before the next addition. Following complete dissolution, the flask was then opened slightly and incubated at 55°C for 1 hr. After cooling, the solution was then precipitated in 20 times excess volume of acetone (4 L), resulting in white solid fibers. The precipitate was then dissolved in ultrapure water, dialyzed, and freeze-dried.

### 2.4. $^{1}$H nuclear magnetic resonance (NMR) characterization of synthesized polymers

DMSO-d6 (6 mg/mL) was used to dissolve gelatin and GelMA and $D_2O$ (10 mg/mL) was used to dissolve HAGM, either was incubated at 50°C overnight. $^{1}$H NMR spectra were recorded by applying 10 sec recycle delay for 64 scans at ambient temperature using a Bruker DRX 400 spectrometer working at 400 MHz. The degree of methacrylation (DM) of GelMA was determined as the percentage of gelatin amino groups (including lysine and hydroxylysine) that were modified in GelMA. The two vinyl protons of the methacrylamide gave rise to two signals peak at $\delta = 5.3$ and 5.6 ppm. The lysine methylene signals (with $\delta = 2.8$ to 2.95 ppm) of non-modified gelatin spectra and GelMA spectra were integrated separately to derive the areas of lysine methylene, according to a previously defined method [25]. The DM of the GelMA was calculated using Eq. 1.

$$\mathrm{DM}(\%) = 1 - \frac{\mathrm{I(lysine\ methylene\ of\ GelMA)}}{\mathrm{I(lysine\ methylene\ of\ gelatin\ without\ modification)}} \times 100 \quad (1)$$

The DM of HAGM was determined by the number of methacryloyl groups presented in every repeating HA disaccharide unit. Vinyl protons of methacrylate groups presented chemical shifts

of 6.2 and 5.15 ppm. The DM of HAGM can therefore be calculated based on the ratio of methyl protons (δ = 1.95 ppm) of methacrylate groups to methyl protons (δ = 2.01 ppm) of amide groups on HA with Eq. 2.

$$\mathrm{DM}\ (\%) = \frac{\mathrm{I_{H'}(methyl\ proton\ on\ GM)\ /\ 3}}{\mathrm{I_H\ (methyl\ proton\ on\ HA)\ /\ 3}} \times 100 \quad (2)$$

**2.5 Preparation of MXF loaded gelatin and GelMA NPs**

Gelatin and GelMA NPs were prepared using a desolvation technique previously reported by Kimura *et al.* [26] with some modifications. A stepwise preparation procedure is depicted in Fig. 1A, and the structure of MXF loaded gelatin/GelMA NPs is shown in Fig. 1B. Briefly, 5% (w/v) of gelatin/GelMA was dissolved in 2 mL of DI water at 45℃ under constant stirring (300 rpm). After complete dissolution, the pH was adjusted to 7.8 at room temperature using 0.1 M NaOH to provide maximum electrostatic interactions between GelMA and the drug candidate. A stock solution of MXF at the concentration of 35 mg/mL was prepared and added to the pH adjusted GelMA solution while stirring. The solution was stirred at 45℃ for 15 min. This step was followed by dropwise addition of 3 mL of acetone (organic phase, served as desolvating agent) at 45℃ under constant stirring (600 rpm) until a faint permanent turbidity was observed. Next, 0.4% (w/v) of glutaraldehyde (GA) and 55 µL of Irgacure 2959 solution (from freshly prepared stock solution of 11 mg/mL) were pipetted into the solution, respectively. The solution was kept stirring at room temperature overnight at 600 rpm and covered with aluminum foil to protect against light. The acetone fraction in the solution was then evaporated using a rotary evaporator (BUCHI

Rotavapor® R-100). The solution containing solidified drug loaded GelMA NPs, was collected in glass vial, and stored at -4°C for further characterization.

### 2.6. Physicochemical characterization of empty and MXF loaded GelMA NPs

#### 2.6.1 Particle size characterization

The hydrodynamic size of NPs was characterized using a Malvern Panalytical dynamic light scattering (DLS) Zetasizer. The bulk suspension of NPs was diluted in Milli-Q $H_2O$ (10 µL of emulsions in 1 mL of Milli-Q $H_2O$) in a plastic 1 cm cuvette. Once the light is shined on the particles, it scatters and shows variance in terms of intensity. The intensities of scattered light and angles of light detectors were recorded and applied to different correlation equations to calculate the diffusion coefficient, *D*. The particle size is then derived using the Stokes-Einstein equation, Eq. 3 [27].

$$D = \frac{\mathrm{kT}}{6\pi\mu\mathrm{r}} \qquad (3)$$

*D* has already been defined as the diffusion coefficient of NPs, k is a physical constant named Boltzmann constant, T is the temperature, µ refers to the viscosity of solvent medium and r is the hydrodynamic radius of particles being measured.

#### 2.6.2 PDI characterization

The PDI characterizes the uniformity of a solution containing NPs, and can be calculated by Eq. 4 [28].

$$\mathrm{PDI} = \left(\frac{\sigma}{2r}\right)^2 \qquad (4)$$

σ refers to the standard deviation of NPs average size distribution and r refers to the hydrodynamic radius of particles. Large PDI value suggests that there is a large size distribution and potential aggregation occurred in NPs solution.

### 2.6.3 Encapsulation efficiency characterization

The encapsulation efficiency of MXF loaded GelMA NPs were determined by diluting the filtrate of the MXF loaded GelMA NPs dispersion with DI water and measuring spectrophotometrically the absorbance at 302 nm using a Thermo Scientific™ NanoDrop™ One/One$^C$ Microvolume UV-Vis spectrophotometer. Standard samples were made by preparing a serial dilution of MXF solution from the MXF stock solution (35 mg/mL) in DI water.

Then the filtrate absorbance for each batch of MXF loaded GelMA NPs was analyzed using a calibration curve and re-calculated for the encapsulated concentration using Eq.5 [29].

$$\text{Encapsultion Efficiency}\ (\%) = \frac{C_{total} - C_{free}}{C_{total}} \times 100 \qquad (5)$$

$C_{total}$ is defined as the total amount of MXF added and $C_{free}$ is the amount of free MXF measured inside the filtrate. The value of $C_{total} - C_{free}$ equals to the drug concentration loaded inside the MXF loaded GelMA NPs.

### 2.6.4 *In vitro* release study

The *in vitro* release profiles of MXF from GelMA NPs were determined by a dialysis method as described previously [30]. Four batches of MXF loaded GelMA NPs with different drug concentration (0.05%, 0.25%, 0.5% and 1% (w/v)) were prepared following the exact same procedure described in section 2.5. Briefly, 1 mL from each batch of MXF loaded GelMA NPs was transferred into dialysis membranes (molecular weight cut-off: 12-14 kDa) and submerged into DPBS buffer (10 mL total volume) inside glass vials with magnetic stirring bars inside. At predetermined time points, 100 µL of sample was taken and replaced with fresh 100 µL of DPBS buffer up to 5 days. The amount of MXF released at each time point was analyzed using a Thermo Scientific™ NanoDrop™ One/OneC microvolume UV-Vis spectrophotometer. At the end of the study, GelMA NPs were collected from the dialysis bag and analyzed for the remaining fraction of MXF entrapped within GelMA NPs, after filtration, using the Thermo Scientific™ NanoDrop™ One/OneC microvolume UV-Vis spectrophotometer.

## 2.7. Preparation of MXF loaded GelMA NPs incorporated GelPatch

A visible light (450-550 nm) photoinitiator (PI) system was utilized to crosslink prepolymers and form adhesive biocompatible hydrogels, GelPatch. The PI system was prepared by dissolving 0.5 mM Eosin Y disodium salt (photoinitiator), 1.875 % (w/v) TEA (co-initiator) and 1.25 % (w/v) VC (co-monomer) in DPBS. The hydrogel prepolymer solution was prepared by dissolving 3% (w/v) of HAGM and 7% (w/v) of GelMA in the PI solution composed of 4:1 (v/v) ratio of TEA/VC to Eosin Y solution, separately. (See Fig. 1B) A batch of MXF loaded GelMA NPs with 0.05% (w/v) MXF was prepared following the procedure described in section 2.5 and added to the

prepolymer solution. 1 M NaOH aqueous solution was used to adjust the pH to 7.4. The prepolymer solution was kept in 45-50℃ incubator overnight and crosslinked for 4 min under exposure to LS1000 Focal Seal Xenon Light Source (1000 mW/cm$^2$, Genzyme).

### 2.8. *In vitro* release study of free MXF and MXF loaded GelMA NPs incorporated GelPatch

Two GelPatch formulations were prepared following the procedure described in section 2.7. Free MXF loaded GelPatch formulation was prepared via direct addition of 0.1 mg of MXF to 500 µL of the GelPatch prepolymer solution and mixed well. The GelMA NPs loaded GelPatch formulation was prepared via addition of 200 µL MXF loaded NP solution (MXF concentration of 0.05% (w/v)), prepared following the procedure described in section 2.5, to 300 µL of the GelPatch prepolymer solution to obtain final amount of 0.1 mg of MXF in 500 µL of solution. After complete dissolution, both formulations were crosslinked for 4 min under exposure to LS1000 Focal Seal Xenon Light Source (1000 mW/cm$^2$, Genzyme). The crosslinked adhesive hydrogels were submerged into glass vials containing 5 mL of DPBS solution. The glass vials were placed on a shaking incubator at controlled temperature of 37°C. Samples were taken at the total volume of 1 mL at predetermined time points and replaced with fresh DPBS for a total time period of 14 days. The concentration of released MXF in the release media (i.e., DPBS) was measured using a Thermo Scientific™ NanoDrop™ One/OneC microvolume UV-Vis spectrophotometer. The absorbance data was then analyzed to obtain the concentrations and consequently the cumulative release profiles. The release data was then fitted based on the non-steady state diffusion model which is governed by Fick's second law Eq.6 [31] and the diffusion coefficient was calculated.

$$\frac{Mt}{M\infty} = 4\sqrt{\frac{Dt}{\pi\lambda}} \quad (6)$$

$M_t$ stands for the amount of drug released from the GelPatch after t min and $M_\infty$ stands for the total amount of drug loaded in GelPatch initially. *D* is the diffusion coefficient; t represents the time, and $\lambda$ stands for the thickness of hydrogel sample.

### 2.9. Mechanical characterization of free drug and NPs incorporated GelPatch

#### 2.9.1 Compression test

70 µL of free MXF and MXF loaded GelMA NPs incorporated GelPatch prepolymer solution prepared in section 2.8 were pipetted into cylindrical polydimethylsiloxane (PDMS) molds (height: 2.5 mm; diameter: 6 mm) and crosslinked for 4 min under exposure to LS1000 Focal Seal Xenon Light Source (1000 mW/cm$^2$, Genzyme). Following the crosslinking, a digital caliper was used to measure the dimensions of hydrogels. An Instron® 5542 mechanical tester was used to conduct compressive test. Dimensions of the hydrogels were entered as parameters into the Instron® combined software, Bluehill® 3. The disk-shaped crosslinked hydrogels were placed in between the base plate and the compression plate. The rate was set at 1 mm/min until automatic failure detected. The slopes of the compressive stress against compressive strain curves (obtained from the linear section of 0.15 to 0.25 mm/mm strain) were recorded and reported as compressive moduli.

### 2.9.2 Tensile test

A 70 µL of free MXF and MXF loaded GelMA NPs incorporated GelPatch prepolymer solution, prepared in section 2.8, were pipetted into rectangular PDMS molds (12 mm x 6 mm x 1 mm) and crosslinked for 4 min under exposure to LS1000 Focal Seal Xenon Light Source (1000 mW/cm$^2$, Genzyme). Tensile test was conducted using an Instron® 5542 mechanical tester. The rectangular crosslinked hydrogels were placed between two pieces of double-sided tape within the instrument tension grips and extended at a speed of 1 mm/min until failure. The tensile strain and stress placed on the hydrogel samples were recorded using a Bluehill® 3 software during the test. The slopes of the stress-strain curves (obtained from the linear section of 0.15 to 0.25 mm/mm strain) were recorded and reported as tensile moduli.

### 2.9.3 *In vitro* burst pressure test

Burst pressure resistance (i.e., collagen sheet adhesive property) of the GelPatch formulations were measured by using the ASTM F2392-04 standard according to a previously reported method [32]. Briefly, collagen sheets made from porcine intestine (4 cm × 4 cm) were placed in between two stainless steel annuli from a custom-built burst pressure device consisting of a metallic base holder, a pressure meter, a syringe dispenser, and a data collector. A hole (diameter: 2 mm) was created through the sheet and was sealed by applying 30 µL of GelPatch prepolymer solution described in section 2.8 and crosslinking via exposure to LS1000 Focal Seal Xenon Light Source (1000 mW/cm$^2$, Genzyme). Next, airflow was applied into the system, and the maximum burst pressure was recorded until the hydrogel detached from the collagen sheet and/or the hydrogel ruptured.

The burst pressure resistance was measured using a pressure sensor (PS-3203, PASCO Scientific, Roseville, CA) connected to a computer.

### 2.9.4 Swelling test

Two formulations of GelPatch prepolymer solution (free MXF and NPs loaded) were prepared as described in section 2.8. 70 µL of each formulation was pipetted into cylindrical PDMS molds (height: 2.5 mm; diameter: 6 mm) and crosslinked for 4 min under exposure to LS1000 Focal Seal Xenon Light Source (1000 mW/cm$^2$, Genzyme). The weight of each crosslinked hydrogel sample was measured immediately after crosslinking and after 24 hr in DPBS at 37°C. The swelling ratio was then calculated according to Eq. 7 [21], where $W_0$ is the weight of the sample after crosslinking and $W_1$ is the final weight of the sample after 24 hr of incubation.

$$\text{Swelling ratio } (\%) = \frac{W_1 - W_0}{W_1} \times 100 \qquad (7)$$

## 2.10 *In vitro* cell studies

Human telomerase-immortalized corneal epithelial (hTCEpi) cells were cultured in an incubator at 37°C in KBM™ basal media (00192151). Cells were seeded on hydrogel scaffold's surfaces according to a previously reported method [33]. In brief, 10 µL of the GelPatch prepolymer solution prepared as described in section 2.8 was spread uniformly on a 3-(trimethoxysilyl) propyl methacrylate (TMSPMA)-coated glass slide and then crosslinked for 4 min under exposure to LS1000 Focal Seal Xenon Light Source (1000 mW/cm2, Genzyme). A surface area of 1 cm x 1 cm was created for crosslinked hydrogels. Hydrogel samples were placed in 24-well tissue culture

plates before hTCEpi cells were seeded on their surfaces (105 cells per sample). After 20 min of incubation of seeded samples at 37℃ supplied with 5% $CO_2$ in a humid incubator, 400 μL of KBM™ basal media was added to each well and incubated. Every other day, the media was changed with fresh KBM™ basal media.

A Live/Dead™ Viability/Cytotoxicity Kit (Invitrogen) was employed to study the viability of cells cultured on the hydrogel scaffolds at day 1 and 3 as explained by the manufacturer's instructions. In short, calcein AM solution at 0.5 μL/mL and ethidium homodimer solution at 2 μL/mL in DPBS were used to stain the cells. Green color was observed for viable cells and red color was observed for dead cells. Hydrogel samples were washed with DPBS buffer solution after incubation for 15 min and the images of cells were captured using a fluorescence optical microscope (ZEISS Primovert). The images captured were analyzed and labeled using ImageJ software. Cell viability (%) was calculated by dividing the number of live cells by the total number of cells (including dead cells).

Proliferation and metabolic activity of cells were characterized with a PrestoBlue assay (Invitrogen). Data was recorded at day 1, 3, and 7 after culture according to the manufacturer's instructions. In brief, a media solution was prepared with 10% (w/v) PrestoBlue reagent. Seeded hydrogel samples were incubated with the media solution at 37℃ supplemented with 5% $CO_2$. A plate reader (BioTek) set at (excitation: 540 nm; emission: 600 nm) was used to determine the fluorescence intensity of the solution.

F-actin filaments and Alexa Fluor 594-phalloidin (Invitrogen) were employed to stain the cells in order to evaluate their morphological characteristics and visualize the cytoskeleton and nuclei more clearly with DAPI. In brief, cells were fixed, permeabilized and blocked by 15 min incubation with 4% (w/v) paraformaldehyde, 10 min incubation with 0.3% (v/v) Triton and 30 min incubation with 1% (w/v) bovine serum albumin (BSA) in DPBS at room temperature, respectively. Hydrogel samples were incubated with phalloidin for 45 min (1:400 dilution) in BSA solution and with DAPI (1:1000 dilution) for 1 min. All samples were washed thoroughly before taken pictures using the ZEISS fluorescent microscope.

### 2.11 Antibacterial studies

#### 2.11.1 Zone of inhibition (ZOI)

Frozen methicillin-resistant *Staphylococcus aureus* (MRSA) and *Pseudomonas aeruginosa* were taken with inoculation loop, streaked on tryptic soy agar plates and incubated at 37℃ for 24 hr. One single isolated colony was chosen and incubated inside tryptic soy broth at 37℃ for 24 hr. The bacteria solution was diluted to 0.5 McFarland which is approximately $1x10^8$ colony forming unit (CFU)/mL using optical density measured at 625 nm wavelength. This solution was streaked on the tryptic soy agar plate for uniform lawn of bacteria. The hydrogels containing with 0.05% (w/v) of MXF loaded NPs were prepared following the same procedure mentioned in section 2.8. The samples were placed on the agar plate. As control, hydrogel samples were prepared following the exact same procedure mentioned in section 2.8 without any MXF loaded. For each bacteria type, 3 replicates were prepared. The agar plates with hydrogels were incubated at 37℃ and the

ZOI was measured every 24 hr for 5 days. The ZOI was recorded by measuring the diameter of bacteria free clear region around the hydrogels using a digital caliper.

### 2.11.2 Measurement of the Colony Forming Unit (CFU)

Frozen MRSA and *Pseudomonas aeruginosa* were taken with inoculation loop, streaked on tryptic soy agar plates and incubated at 37℃ for 24 hr. One single isolated colony was taken and incubated inside tryptic soy broth at 37℃ for 24 hr. The bacteria solution was diluted to $1x10^8$ CFU/mL using optical density measured at 625 nm wavelength. The resulting bacteria solution was serially diluted in tryptic soy broth over a 2-log range to a density of $1x10^6$ CFU/mL. Hydrogels, prepared following the same procedure described in section 2.8 with MXF loaded NPs and without MXF, were placed in 48-well plates and sterilized under UV light for 10 min. Each hydrogel sample was seeded with 2 mL of each type of bacteria solution and incubated at 37℃ for 24 hr. One mL of bacterial solution was taken from each incubated sample well and diluted with tryptic soy broth to 3-log range. Then, 100 µL of the solution was added to each agar plate and uniformly spread over it. The agar plates were incubated for 24 hr and the colonies on each plate were counted and recorded. CFU were calculated based on dilution factor of 1000.

## 2.12 Statistical Analysis

For every experiment, at least three samples were prepared and tested for results. Data were presented in the format of means ± SD (*: $P < 0.05$, **: $P < 0.01$, ***: $P < 0.001$, ****: $P <$

0.0001). One-way or two-way analysis of variance (ANOVA) *t* test was performed for statistical analysis (GraphPad Prism 8.0.2, GraphPad Software).

## Chapter 3. Results and Discussion

The MXF loaded GelMA NPs were formed following the stepwise procedure shown in Fig. 1A. To form the GelPatch hydrogel, 3% (w/v) of HAGM and 7% (w/v) of GelMA were dissolved in DPBS solution containing TEA, VC and Eosin Y as initiators. The formulated prepolymer solution was then mixed with the MXF loaded GelMA NPs and photopolymerized by exposing to visible light (Fig. 1B)

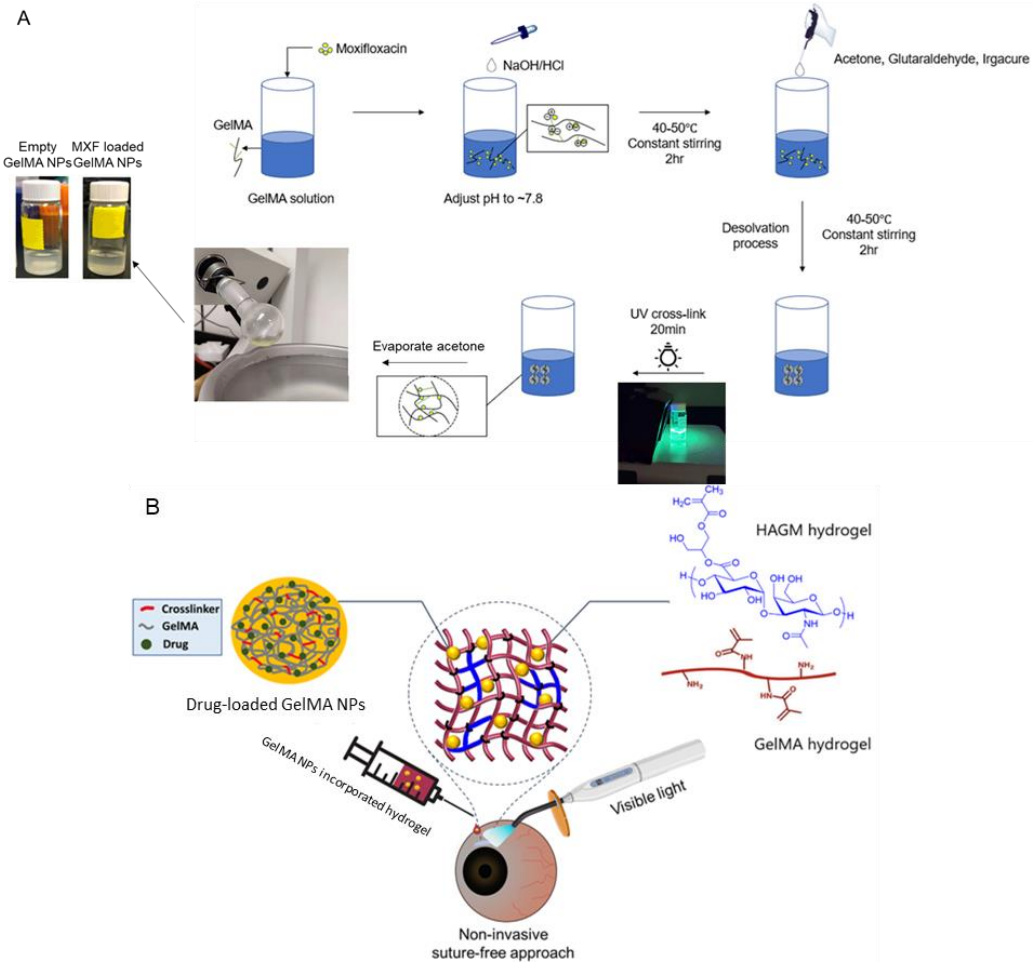


**Fig. 1.** Synthesis and application of GelPatch adhesive hydrogels loaded with MXF loaded GelMA NPs. (A) Stepwise schematic of the preparation procedure of MXF loaded GelMA NPs. (B) Schematic of the formation and application for MXF loaded GelMA NPs incorporated GelPatch.

### 3.1 Physicochemical characterization of gelatin/GelMA NPs

Gelatin/GelMA NPs formulations were optimized based on polymer type, concentration and crosslinker concentration. Solvent desolvation technique is one of the most applied methodology to form NPs. However, inconsistency in the literatures regarding NPs diameter, PDI and experimental methods exists [34]. Therefore, one focus of this study was to perform a systematic study to check for the impact of variables on formed particle size and PDI.

Previous studies have shown that ocular nano delivery systems in the form of suspension, can lead to improved drug bioavailability with smaller particle sizes within the range of about 10 to 150 nm [35]. Smaller particle sizes help with enhanced penetration through the tear film and the mucin layer on the eye. Current strategies based on the use of NPs for drug delivery focuses on NPs entrapment (chemical and physical) within the matrix of the hydrogel patch, and diffusion (i.e., slow release) of hydrophilic drug molecules from the particles to the hydrogel matrix (primary interface) and from the hydrogel matrix to the outside media (secondary interface). In order to have better drug eluting effect, a small NP size is desirable. In addition, a small PDI value ensures that NPs do not aggregate in a solution. Therefore, a particle diameter of 150 to 250 nm and a PDI value < 0.2, were considered to be within the acceptable range for this study [36].

Four batches of gelatin and/or GelMA NPs based on different polymer concentrations and molecular weights were prepared. An average size of 158.5 ± 15.5 nm, 283.8 ± 27.5 nm, 205 ± 3 nm and 232.7 ± 35 nm were obtained for 5% (w/v) gelatin (5% Gelatin), 5% (w/v) high DM GelMA (5% H-GelMA), 10% (w/v) high DM GelMA (10% H-GelMA) and 10% (w/v) low DM

GelMA (10% L-GelMA), respectively (Fig. 2, A and F). The 5% Gelatin batch had significantly ($P < 0.001$) smaller particle size compared to the 5% H-GelMA batch. However, the PDI for 5% Gelatin was 0.28 ± 0.05, which means that the NP size distribution was within a wide range, which is undesirable for homogeneous NPs distribution within the polymer matrix and drug release. The particles formed by using 10% H-GelMA showed a smaller average particle size as compared to 5% H-GelMA ($P < 0.05$). also, 10% H-GelMA batch had a PDI of 0.156 ± 0.01, indicating better uniformity of NP size distribution. The particles formed by using 10% L-GelMA were not ideal in both size and PDI (0.42 ± 0.03) (Fig. 2, A and B). Based on the obtained results, we decided to continue with the formulation of NPs composed of 10% H-GelMA, since the size and PDI fit well our predefined range.

GA is a chemical crosslinker that we used for the formulation NPs [37]. In this study, the applied various concentrations of GA ranging from 0.0 to 0.8 %(v/v). The selected GA range is adjusted relative to the applied concentration of GelMA in the solution [38]. The GelMA concertation was 10% H-GelMA based on the results shown in the previous section. The results showed correlation between increase in GA concentration from 0 to 0.8% and decrease in average size of the NPs from 347.8 ± 39.9 nm to 166.5 ± 7.7 nm (Fig. 2, D and G). In details, an increase in GA concentration from 0.2 to 0.4% resulted a significant ($P < 0.001$) increase in NPs size from 325.8 ± 22.2 nm to 208.9 ± 0.02 nm. Similar correlation was observed with PDI as well (Fig. 2E). An increase in GA concentration from 0 to 0.4% resulted in decrease in PDI from 0.91 ± 0.13 to 0.1 ± 0.02, respectively (Fig. 2, E and G). However, at GA concentration of 0.8%, an increase in PDI up to 0.32 was observed. In general, the aldehyde groups of GA interact with the hydroxyl and/or amine groups of GelMA molecules and form intermolecular crosslinking within the entangled

GelMA chains due to the induced desolvation by acetone. We hypothesize that an increase in GA concentration above 0.4%, apart from increasing the density of crosslinking, also causes intramolecular crosslinking among particles in the solution which appeared as an increase in PDI. Based on predefined range for PDI and sizes of the GelMA NPs, GA concentration of 0.4% was selected to crosslink the NPs.

Surface charge density (zeta potential) of GelMA NPs was measured using a Malvern Panalytical Zetasizer. The results showed that polymer chain length and/or concentrations of polymer had no significant impact on overall surface charge density. Measured zeta potential values of formulated NPs varied between -4.95 mV and -5.56 mV (Fig. 2C).

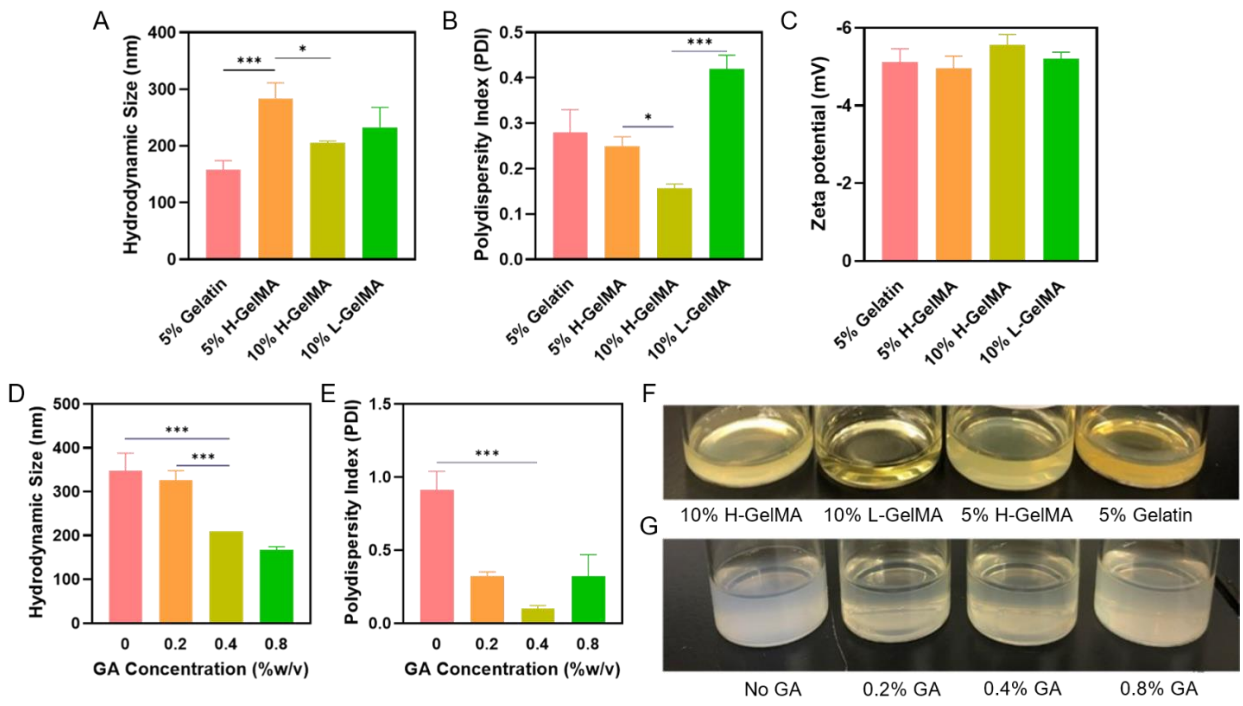


**Fig. 2.** Physicochemical characterization of gelatin/GelMA NPs. Effect of polymer type and concentration on (A) hydrodynamic size, (B) PDI, and (C) zeta potential of the NPs. Effect of GA concentration on (D)

hydrodynamic size and (E) PDI of the NPs. (F) Visual comparison among NP solutions made of different polymer and concentration. G) Visual comparison among NP solutions made of GelMA and various GA concentrations. Data are reported as means ± SD (*: $P < 0.05$, **: $P < 0.01$, ***: $P < 0.001$, ****: $P < 0.0001$; $n \geq 3$).

### 3.2 Physicochemical characterization of MXF loaded GelMA NPs

Based on the obtained results from the previous optimization step, we continued with the NPs formulation composed of 10% of H-GelMA and 0.4%. GA. Previous studies have shown loading of MXF at the concentration of 1% (w/v) into chitosan-dextran NPs, as an ocular drug delivery system, increased MXF ocular bioavailability compared to free MXF application [37]. In our study, different formulations of MXF loaded NPs were prepared based on varying concentration of MXF from 0.05 to 1% (w/v). Results based on physicochemical characterization showed no significant difference on size, PDI and zeta potential of different formulations (Fig. 3, A-C). The overall average size of the NPs varied between 210 to 224 nm. The measured values of PDI varied between 0.17 to 0.22. The average zeta potential remained around -5.00 mV for all the formulations, indicating that the addition of drug molecule (at its charged state) did not change the surface charge density of particles.

Encapsulation efficiency of four different formulations based on varying concentration of MXF from 0.05 to 1% (w/v) was analyzed as descried previously in section 2.6.3. The results showed that, increasing drug loading decreased the encapsulation efficiency. When the concentration of drug molecules increases, the number of interacted molecules with the charged GelMA backbone

tends to decrease gradually and maintains at a fixed level after reaching the maximum loading capacity of NPs. The encapsulation efficiency for the 0.05% (w/v) MXF loaded NPs formulation was 93.8 ± 8.2% which correlated with 0.47 mg/mL of MXF (Fig. 3, D-E). With an increase in MXF to above 0.5% (w/v), the encapsulation efficiency dropped to an average of 60.79 ± 2.90% which correlated with 3.04 mg/mL of MXF (Fig. 3, D-E). Since both batches contain the same number of NPs, we concluded that most of NPs were loaded with MXF and the maximum loading capacity was achieved at 0.05% (w/v) of MXF. Considering the minimum inhibitory concentration (MIC) for MXF is less than 0.25 µg/mL and 1 µg/mL against *Staphylococcus aureus* and *Pseudomonas aeruginosa*, respectively, the formulation loaded with 0.05% (w/v) MXF or above can be considered as an optimized formulations to deliver the therapeutic level of MXF to the injured ocular tissue.

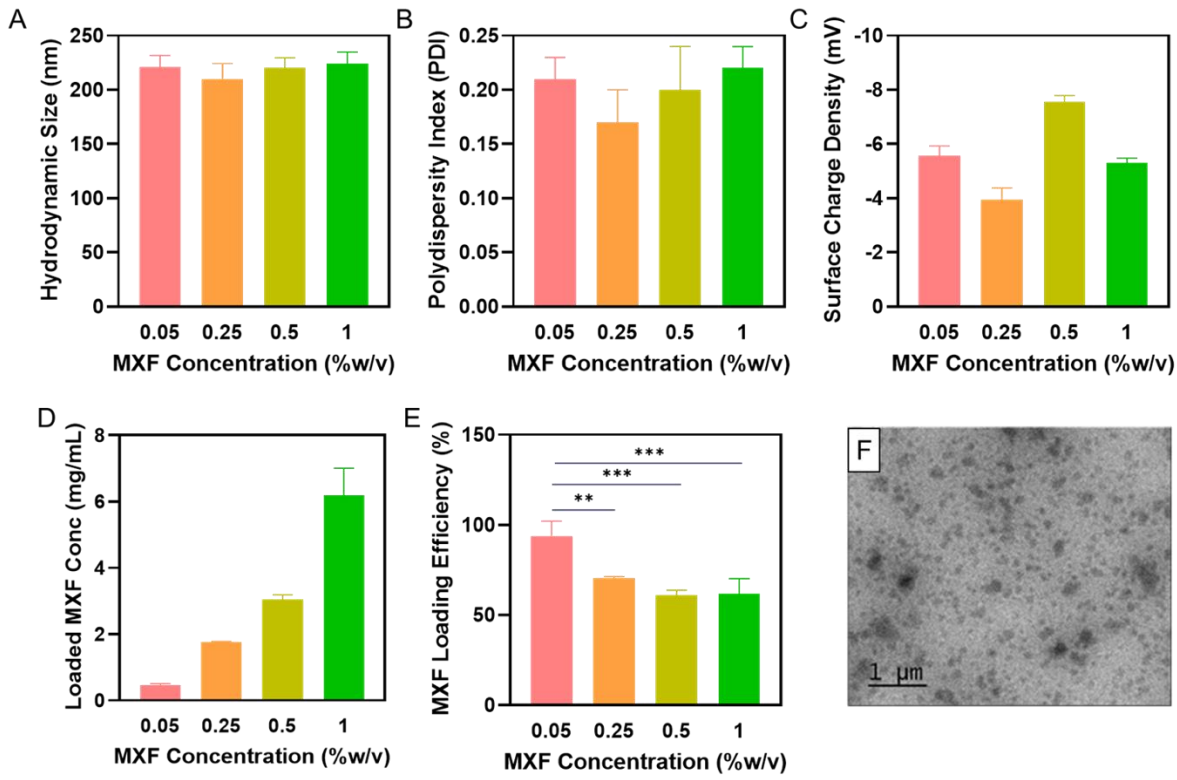


**Fig. 3.** Physicochemical characterization of MXF loaded GelMA NPs (the particle was formed using 10% H-GelMA/0.4% GA with different amount of MXF). Effect of drug loading on (A) hydrodynamic size, (B) PDI, and (C) surface charge density of the NPs. Effect of drug loading on (D) loaded MXF concentration of NPs and (E) MXF loading efficiency of NPs. (F) A representative TEM image of MXF loaded NPs in DI water. Data are reported as means ± SD (*: $P < 0.05$, **: $P < 0.01$, ***: $P < 0.001$, ****: $P < 0.0001$; $n \geq 3$).

### 3.3 *In vitro* release studies on MXF loaded NPs and NPs incorporated GelPatch

#### 3.3.1 *In vitro* cumulative release study on MXF loaded NPs

As explained in section 2.6.4, the *in vitro* release study was carried out via dialyzing GelMA NPs suspensions against DPBS. The *in vitro* release profile of 0.05% (w/v) MXF from GelMA NPs is

shown in Fig. 4A. This Figure shows that about 32.31 ± 2.56% of MXF was released from the NPs during the first 2 hr. MXF was then slowly released from NPs, reaching to 98.5 ± 0.59% at day 5. With the formulations of NPs loaded with 0.25 to 1% (w/v) of MXF, more prominent burst release was observed as compared with the formulation loaded with 0.05% (w/v) of MXF. During the first 2 hr, a burst release of 44.72 ± 3.12%, 45.46 ± 3.68% and 40.53 ± 1.25% was observed for formulations loaded with 0.25%, 0.5% and 1% (w/v) of MXF, respectively. The burst release was followed by the sustained release of MXF up to 95.52 ± 1.44%, 97.75 ± 1.45% and 84.55 ± 2.16% on day 14 for the formulations loaded with 0.25%, 0.5% and 1% (w/v) of MXF, respectively. In general, the results showed that GelMA NPs loaded with 0.05% (w/v) drug led to a higher burst release compared to the 0.05% (w/v) MXF. This was primarily due to the existence of non-entrapped/non-interacted MXF in the formulation and only the fraction of MXF which underwent the charge-charge interactions showed the sustained release profile. In addition, the hydrophilic nature of GelMA can facilitate burst release profile via incorporation of water molecules from surrounding aqueous solution and promote the release of hydrophilic MXF molecules which are close to the aqueous/polymer interface of NPs [39].

### 3.3.2 *In vitro* cumulative release study on NP incorporated GelPatch

GelPatch was introduced as a platform for our ocular drug delivery system. As described in section 2.7, GelPatch is composed of GelMA and HAGM. Based on the $^{1}$H NMR analysis, the DM of GelMA was calculated to be 61% using Eq. 1 and the DM of HAGM was calculated to be 11% using Eq. 2.

Based on the results from *in vitro* release of different formulations, we chose the GelMA NPs formulation composed of 0.05% (w/v) MXF to be loaded inside the GelPatch as drug delivery platform in order to obtain slow release of MXF to the ocular tissue upon hydrogel adhesion to the tissue. As a control group, we applied GelPatch directly loaded with free MXF in order to evaluate the release profile of our GelMA NPs incorporated GelPatch in the release media (i.e., DPBS). The control group showed a 74.7 ± 2.38% burst release of free MXF from the hydrogel patch within the first 2 hr of incubation. The remaining fraction was released within 24 hr (Fig. 4B). However, The GelPatch formulation incorporated with MXF loaded GelMA NPs showed a burst release of around 29.65 ± 2.65% of MXF during the first 2 hr, and the remaining amount MXF was slowly released into the surrounding media over a time period of 5 days.

The release data was fitted based on the non-steady state diffusion model which is characterized by Fick's second law as described in section 2.8. Fig. 4C shows the cumulative release profile in the form of fraction of drug released ($M_t/M_\infty$) as the function of square root of time. The diffusion coefficient *D* for each GelPatch formulations was calculated based on Fick's second law and the slope of the plotted data (Table. 1). The diffusion coefficient for MXF loaded GelMA NPs incorporated GelPatch is around 1/6 of that for free MXF loaded GelPatch, confirming that the interactions among drug, NPs and hydrogel network were responsible for the sustained release of MXF from GelMA NPs incorporated GelPatch. Similar conclusion was also drawn for the release of methylene blue and caffeine from a supramolecular hydrogel developed previously [31].

Previous studies on the release of MXF and/or highly hydrophilic, charged, small molecules have shown fast release kinetics within the first hr of incubation inside the release media [31]. Our result is the proof of concept that GelPatch matrix as secondary interface can improve the release rate of a hydrophilic drug molecule, MXF, from the GelMA NPs, as compared to the freely loaded MXF inside the GelPatch. It is important to note that the conventional ocular antibacterial therapeutics regimen is based on high dose drug delivery within the first 24 hr, followed by lower dose for at least one weeks [40]. Therefore, our developed formulation has the release kinetics which fits well for the ocular therapeutic purposes.

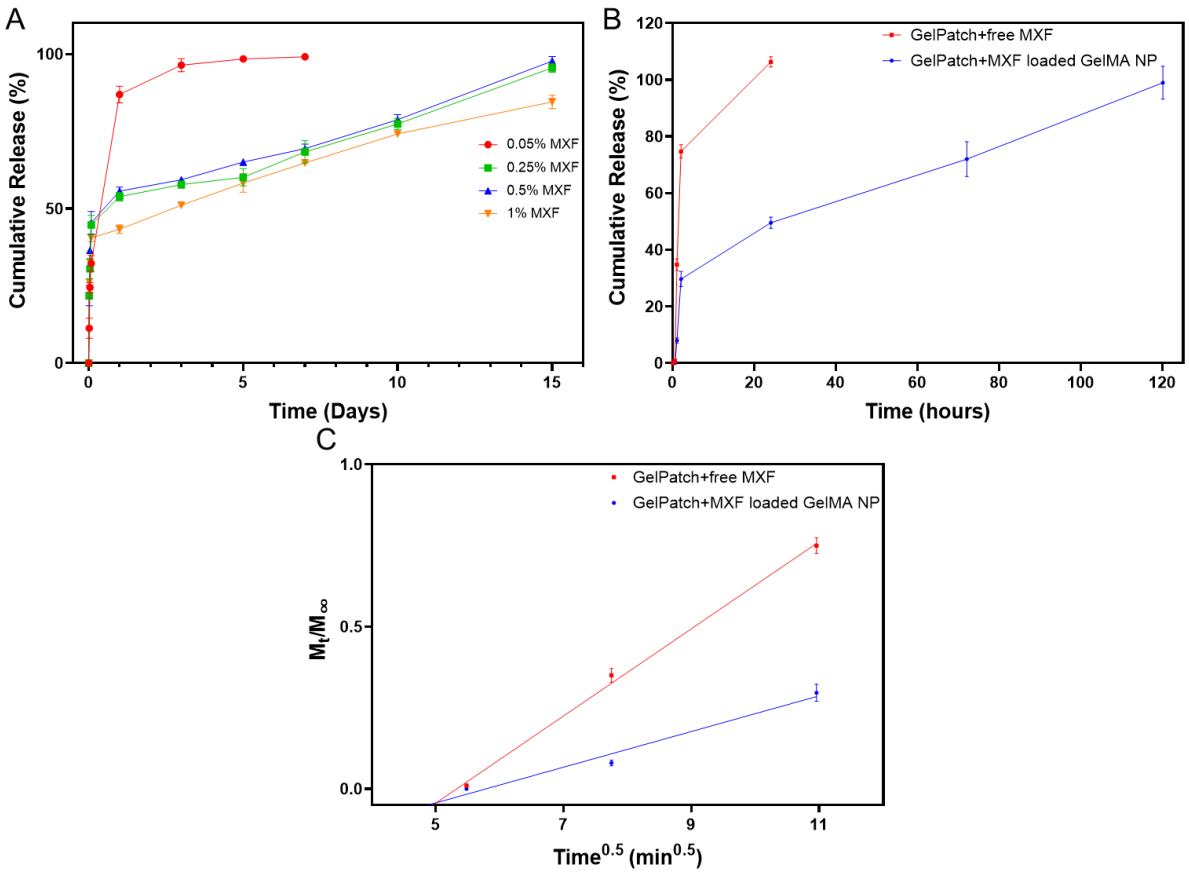


**Fig. 4.** *In vitro* cumulative release profile and kinetics. (A) *In vitro* cumulative release study of 0.05%, 0.25%, 0.5% and 1% (w/v) of MXF loaded GelMA NPs. (B) *In vitro* cumulative release study of MXF

loaded NPs incorporated GelPatch and free MXF loaded GelPatch. (C) Release kinetics for free MXF loaded GelPatch and MXF loaded GelMA NPs incorporated GelPatch (fraction of MXF released vs. square root of time over 5 days.

**Table 1.** Diffusion coefficients of MXF from free MXF loaded GelPatch and MXF loaded GelMA NPs incorporated GelPatch

| **Formulations** | GelPatch+ free MXF | GelPatch+ MXF loaded GNP |
|---|---|---|
| **Diffusion Coefficient ($10^{-10}$ $m^2 \cdot s^{-1}$)** | 17.788±1.146 | 3.049±0.446 |

### 3.4 Mechanical characterization of MXF loaded GelMA NPs incorporated GelPatch

#### 3.4.1 Compressive test

Compressive tests were conducted for three GelPatch formulations, GelPatch, GelPatch loaded with free MXF and MXF loaded GelMA NPs incorporated GelPatch. Fig. 5, A and C show the compressive modulus of the three hydrogel samples. The loading of free MXF in GelPatch increased the compressive modulus from 11.26 ± 2.64 kPa foe pure GelPatch to 28.97 ± 2.38 kPa for GelPatch loaded with free MXF. The incorporation of MXF loaded GelMA NPs increased the compressive modulus of GelPatch more significantly, reaching 40.47 ± 2.71 kPa. We hypothesize that the addition of GelMA NPs increased the crosslinking density of the GelPatch formulation, therefore, compressive modulus was enhanced [41]. Fig. 5B presents the compressive ultimate stress values. Among three formulations of GelPatch, the batch loaded with free MXF showed

significantly higher ultimate stress of 701.33 ± 127.4 kPa. This can be explained by the presence of MXF aggregation inside the GelPatch. For GelPatch and GelMA NPs incorporated GelPatch, we obtained an ultimate stress of 276 ± 15.52 kPa and 261.54 ± 153.70 kPa, respectively.

### 3.4.2 Tensile test

Tensile tests were performed for the three formulations of GelPatch described above. Fig. 5D demonstrated that the loading of GelMA NPs increased the tensile modulus of GelPatch from 32.92 ± 3.64 kPa to 42.75 ± 2.03 kPa, which could be attributed to the higher crosslinking density. Fig. 5, E-F shows the tensile ultimate stress and strain of the hydrogel samples before failure. No significant difference was observed in the ultimate tensile stress among the three hydrogel formulations, ranging from 16.85 to 20.36 kPa.

### 3.4.3 Burst pressure test

Burst pressure tests were conducted to study the hydrogel's adhesive properties to the tissue (Fig. 5, G-I). Bioadhesive hydrogels have superior ability to seal defect or injured sites on the cornea [42]. The burst pressure results for GelPatch and free MXF loaded GelPatch were 26.3 ± 2.3 kPa and 24.5 ± 0.3 kPa, respectively, confirming that free MXF did not affect hydrogel's adhesive properties. After incorporating GelMA NPs into GelPatch, the burst pressure showed 60% increase to 40.8 ± 4.2 kPa as compared with GelPatch and free MXF loaded GelPatch. The burst pressure data for GelMA NPs loaded GelPatch was similar to our previous work on engineering gelatin-based bioadhesive for sealing ocular injures [43]. The engineered MXF loaded GelMA NPs

incorporated GelPatch demonstrated higher burst pressure resistance than commercially available products such as CoSEAL and Evicel, which had burst pressure values of 1.6 ± 0.2 kPa and 1.5 ± 0.7 kPa, respectively [43].

### 3.4.4 Swelling ratio test

Swelling ratios of three GelPatch formulations are reported in Fig. 5H. The GelPatch sample had an average swelling ratio of 13.05 ± 3.69%. After incorporating GelMA NPs, the average swelling ratio decreased to 7.72 ± 2.39%, yet no statistical difference was found. The decrease in swelling ratio can also be explained by increasing crosslinking density in GelPatch containing GelMA NPs. Similar trends were reported by Yihu Wang [44]. For ophthalmic applications, a small swelling ratio of hydrogel is preferred because it can prevent building up of pressure and inflammation at corneal injury sites [44].

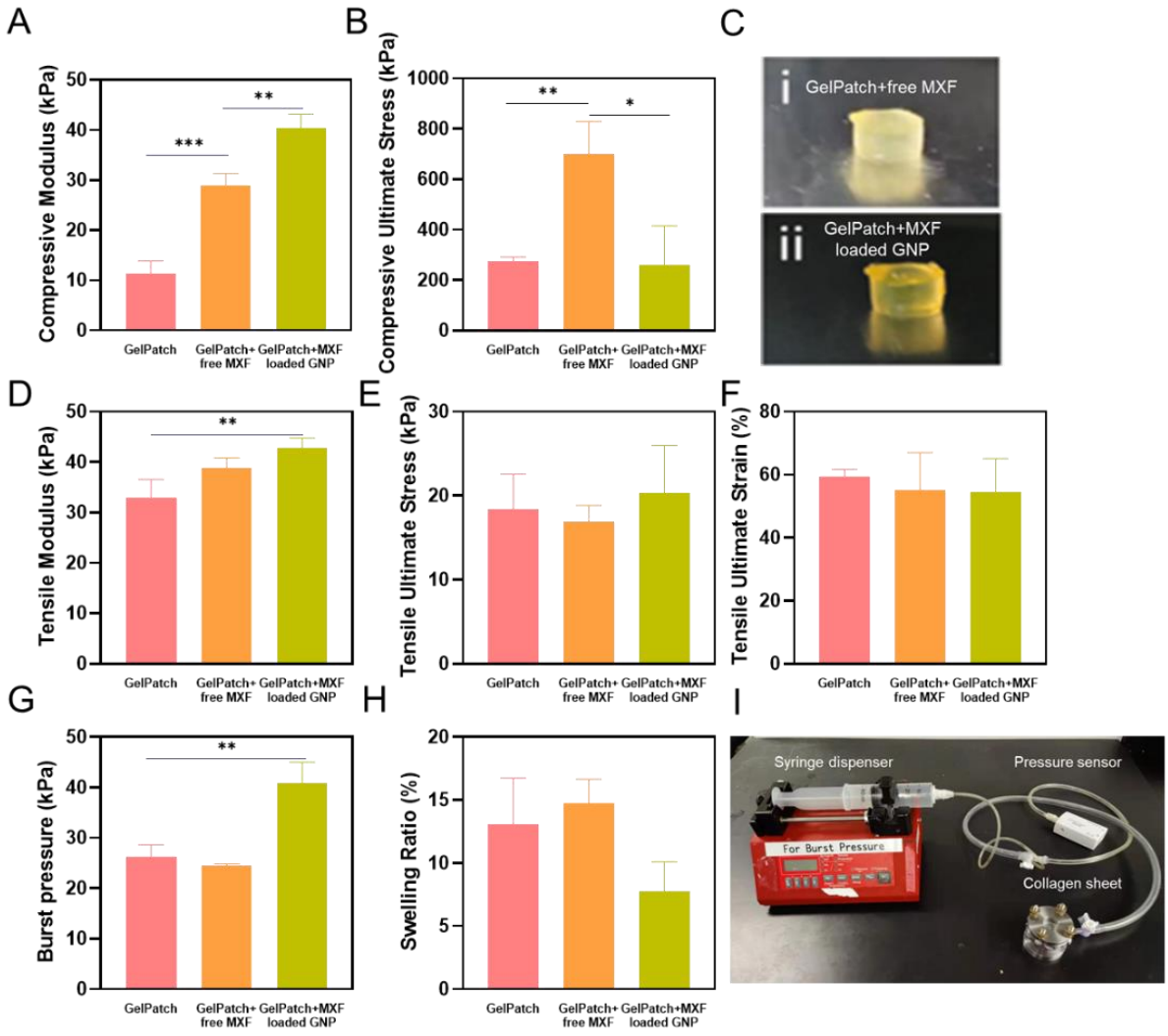


**Fig. 5.** Physical Characterization for three GelPatch formulations (GelPatch, GelPatch loaded with free MXF and MXF loaded GelMA NPs incorporated GelPatch). (A-B) Compressive modulus and ultimate stress of hydrogels. (C) Pictures of free MXF loaded GelPatch and MXF loaded GelMA NPs incorporated GelPatch. (D-F) Tensile modulus, ultimate stress and ultimate strain of hydrogels. (G) Burst pressure and (H) Swelling ratio after 24 hr immersion in DPBS solution. (I) Burst pressure instrument setup.

### 3.5 *In vitro* biocompatibility of the MXF loaded GelMA NPs incorporated GelPatch

The viability as well as the metabolic activity of seeded cells on hydrogel samples were investigated via PrestoBlue and Live/Dead assay at day 1, 3 and 7. These results can be used to evaluate the biocompatibility of GelMA NPs incorporated GelPatch. Micrographs of stained cells derived from Live/Dead assay showed a high viability (> 90%) of cells seeded on either GelPatch or GelMA NPs incorporated GelPatch at day 1 and 3 which was at the early stage of culture (Fig. 6, A-B). Fluorescent staining F-actin was employed to help visualize the morphology of cells at day 1 and 3 cultured on GelPatch formulations. From Fig. 6C, micrographs showed that the cells were able to spread, adhere, extend and proliferate on surfaces of both GelPatch and GelMA NPs incorporated GelPatch which indicated that GelPatch loaded with NPs had good biocompatibility for cell adherence and growth. Furthermore, the metabolic activity of cultured hTCEpi cells were examined through PrestoBlue assay on hydrogel samples. A consistent increase in fluorescence level over 7 days, without a significant difference to the GelPatch, confirmed the cytocompatibility of the GelMA NPs incorporated GelPatch (Fig. 6D).

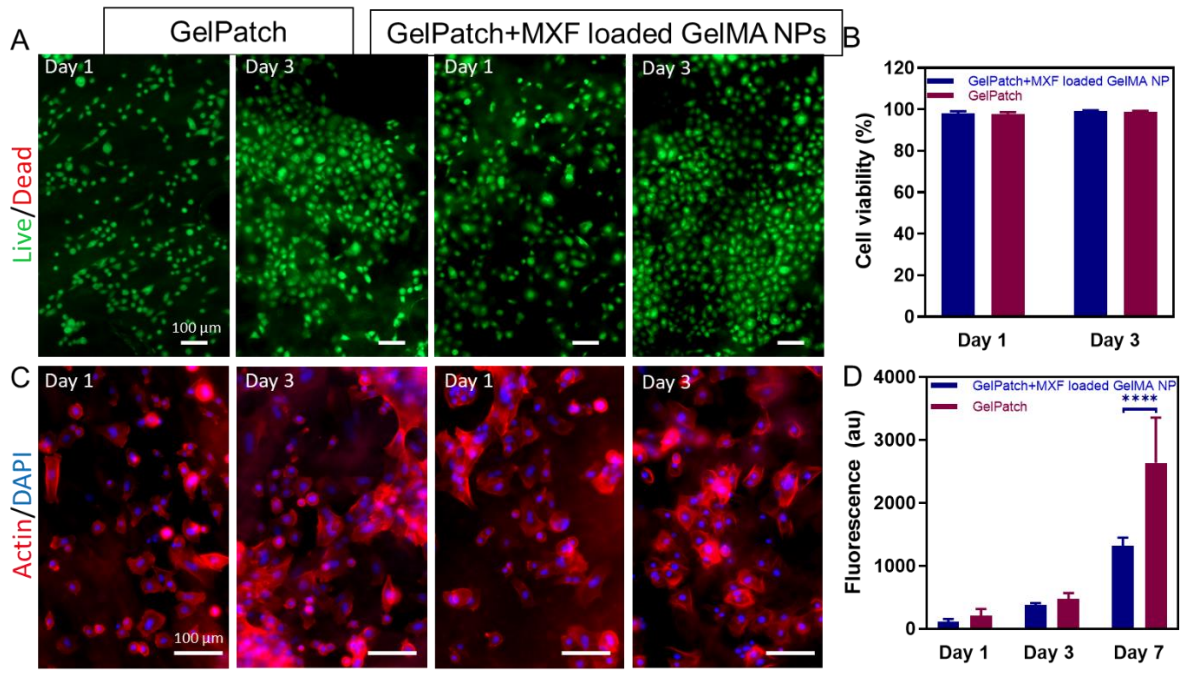


**Fig. 6**. *In vitro* biocompatibility and cytotoxicity tests. (A-B) Live/Dead assay and PrestoBlue assay at days 1 and 3 for GelPatch and MXF loaded GelMA NPs incorporated GelPatch. (C) Fluorescent staining F-actin for cytoskeleton of cells after 1 and 3 days of post-seeding. (D) Fluorescence level (representing the enzymatic activity) of cells after 1, 3 and 7 days of post-seeding.

### 3.6 *In vitro* antibacterial effect evaluation of GelPatch incorporated with MXF loaded NPs

Antibacterial studies were performed using formulations of MXF loaded GelMA NPs incorporated GelPatch and GelPatch. From Fig. 7A, ZOI was observed around MXF loaded GelMA NPs incorporated GelPatch for both types of bacteria *Staphylococcus aureus* (gram-positive) and *Pseudomonas aeruginosa* (gram-negative) seeded on agar plates [45]. There was negligible area of ZOI formed around GelPatch samples, indicating that the GelPatch formulation does not contain any antibacterial components. The diameters for ZOI formed were measured by digital caliper every day and reported in Fig. 7, B to C. The ZOI shown against *Pseudomonas aeruginosa* was

measured to be more than 30 mm for all measurements over 5 days. This value of ZOI represents great antimicrobial effect of the MXF loaded GelMA NPs incorporated GelPatch [46]. For the case of *Staphylococcus aureus*, the diameter was measured to be more than 28 mm for all measurements over 5 days. These results demonstrated that the antibiotics, MXF, released from NPs incorporated in GelPatch had antibacterial effects against both gram-positive and gram-negative bacteria and the release can last for 5 days. The antimicrobial activity was also verified by counting CFU. CFU for MXF loaded GelMA NPs incorporated GelPatch placed on agar plates seeded with *Staphylococcus aureus* and *Pseudomonas aeruginosa* were calculated to be 95 ± 18.38 and 82 ± 50.91 (unit: $1x10^4$ CFU/mL), respectively. Around 1/10 of the value obtained for the control group with GelPatch only samples placed on agar plates.

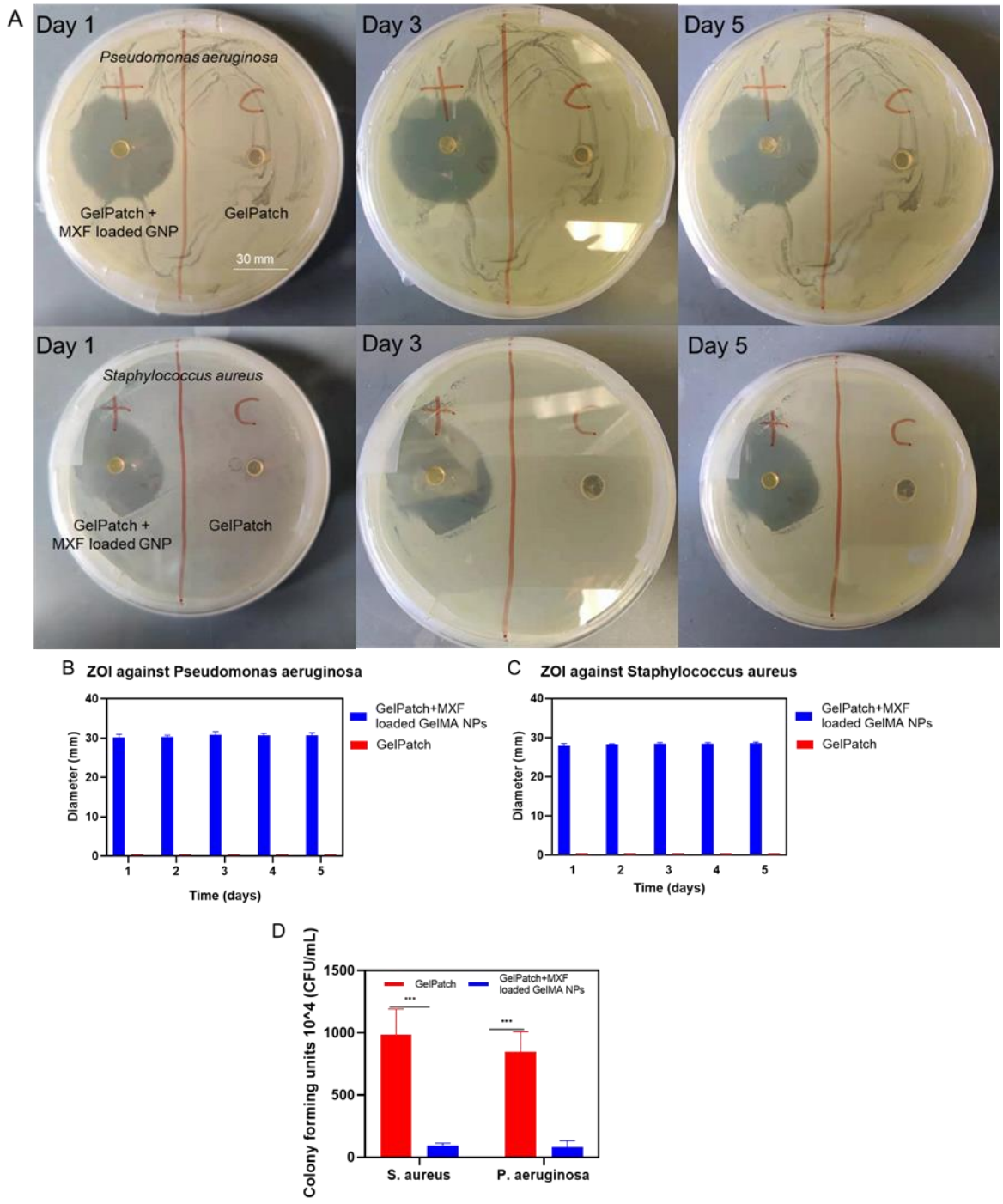


Fig. 7. *In vitro* antibacterial effects of MXF loaded GelMA NPs incorporated GelPatch. (A) Selected images of bacteria grown on agar plates for GelPatch with and without MXF loaded GelMA NPs. (B-C)

Quantitative characterization for ZOI with GelMA NPs incorporated GelPatch placed on agar plates seeded with *Pseudomonas aeruginosa* and *Staphylococcus aureus* bacteria. (D) Quantitative characterization of CFU concentration for GelPatch with MXF loaded GelMA NPs placed on agar plates seeded with *Pseudomonas aeruginosa* and *Staphylococcus aureus* bacteria.

## Chapter 4 Conclusion

We have successfully prepared GelMA NPs by desolvation technique and loaded with MXF, which is effective against eye diseases caused by bacterial infection. Our optimized MXF loaded GelMA NPs batches had an average size range of 210-224 nm with high drug encapsulation efficiency of 93.8%.

A controlled release of MXF from NPs solution and NPs incorporated in GelPatch was observed following the initial fast release in the *in vitro* release experiments. MXF loaded GelMA NPs also enhanced GelPatch's mechanical properties such as elastic modulus and burst pressure. Antibacterial tests revealed that GelPatch with MXF loaded NPs inhibited microbial growth on agar plates for two different bacteria. ZOI maintained at 28-30 mm over a period of 5 days.

We believe that current results have demonstrated the potential of using antibiotics loaded GelMA NPs to treat bacterial infection on eyes. With further studies on *ex-vivo* characterization and optimization for pharmacokinetics and pharmacodynamics, the future of translating this technology into real world biomedical applications is promising.

**Bibliography**


1. J.W.e.a. Yau, Global prevalence and major risk factors of diabetic retinopathy, Diabetes Care, 35 (2012) 556–564.
2. R.K. Klein, B. E., The prevalence of age-related eye diseases and visual impairment in aging: current estimates., Invest. Ophthalmol. Vis. Sci., 54 (2013).
3. Y.C.e.a. Tham, Global prevalence of glaucoma and projections of glaucoma burden through 2040: a systematic review and meta-analysis, Ophthalmology & Visual Science, (2014) 2081–2090.
4. Durand, Marlene L. "Bacterial and Fungal Endophthalmitis." Clinical microbiology reviews vol. 30,3 (2017): 597-613. doi:10.1128/CMR.00113-16.
5. American Academy of Ophthalmology Cornea/External Disease Panel. Preferred Practice Pattern® Guidelines. Bacterial Keratitis.external icon San Francisco, CA: American Academy of Ophthalmology; 2013.
6. Azari, Amir A, and Amir Arabi. "Conjunctivitis: A Systematic Review." Journal of ophthalmic & vision research vol. 15,3 372-395. 6 Aug. 2020, doi:10.18502/jovr. v15i3.7456.
7. Smith, Andrew F, and Curtis Waycaster. "Estimate of the direct and indirect annual cost of bacterial conjunctivitis in the United States." BMC ophthalmology vol. 9 13. 25 Nov. 2009, doi:10.1186/1471-2415-9-13.
8. Jewell, Tim. "8 Common Eye Infections and How to Treat Them." Healthline, 3 Dec. 2018, www.healthline.com/health/infected-eye.

9. Agrahari, Vibhuti et al. “A comprehensive insight on ocular pharmacokinetics.” Drug delivery and translational research vol. 6,6 (2016): 735-754. doi:10.1007/s13346-016-0339-2.
10. Patel, Ashaben et al. “Ocular drug delivery systems: An overview.” World journal of pharmacology vol. 2,2 (2013): 47-64. doi:10.5497/wjp. v2.i2.47.
11. Gaudana, Ripal et al. “Recent perspectives in ocular drug delivery.” Pharmaceutical research vol. 26,5 (2009): 1197-216. doi:10.1007/s11095-008-9694-0.
12. Vrinda Gote, Sadia Sikder, Jeff Sicotte and Dhananjay Pal, Journal of Pharmacology and Experimental Therapeutics September 1, 2019, 370 (3) 602-624; doi: https://doi.org/10.1124/jpet.119.256933.
13. Jessica, Steen. “Contemporary Prescribing of Oral Medications in Eye Disease”. 8 Nov. 2019, NSU College of Optometry.
14. Ji Eun Lee, Nohyun Lee, Taeho Kim, Jaeyun Kim, and Taeghwan Hyeon, Multifunctional Mesoporous Silica Nanocomposite Nanoparticles for Theranostic Applications, Accounts of Chemical Research 2011 44 (10), 893-902, doi:10.1021/ar2000259.
15. Hong, Seyoung et al. “Protein-Based Nanoparticles as Drug Delivery Systems.” Pharmaceutics vol. 12,7 604. 29 Jun. 2020, doi:10.3390/pharmaceutics12070604.
16. García-Pinel, Beatriz et al. “Lipid-Based Nanoparticles: Application and Recent Advances in Cancer Treatment.” Nanomaterials (Basel, Switzerland) vol. 9,4 638. 19 Apr. 2019, doi:10.3390/nano9040638.
17. Anitha Ethirajan, Katrin Schoeller, Anna Musyanovych, Ulrich Ziener, and Katharina Landfester, Synthesis and Optimization of Gelatin Nanoparticles Using the Miniemulsion Process, Biomacromolecules 2008 9 (9), 2383-2389, doi: 10.1021/bm800377w.

18. Kushibiki T, Matsuoka H, Tabata Y. Synthesis and physical characterization of poly (ethylene glycol)-gelatin conjugates. Biomacromolecules. 2004 Jan-Feb;5(1):202-8. doi: 10.1021/bm0343139. PMID: 14715027.
19. Zwiorek K, Kloeckner J, Wagner E, Coester C. Gelatin nanoparticles as a new and simple gene delivery system. J Pharm Pharm Sci. 2005 Feb 3;7(4):22-8. PMID: 15850545.
20. Babita Gaihre, Myung Seob Khil, Douk Rae Lee, Hak Yong Kim, Gelatin-coated magnetic iron oxide nanoparticles as carrier system: Drug loading and in vitro drug release study, International Journal of Pharmaceutics, Volume 365, Issues 1–2, 2009, Pages 180-189, ISSN 0378-5173, https://doi.org/10.1016/j.ijpharm.2008.08.020.
21. Sara Azizian, Afra Hadjizadeh, Hassan Niknejad, Chitosan-gelatin porous scaffold incorporated with Chitosan nanoparticles for growth factor delivery in tissue engineering, Carbohydrate Polymers, Volume 202, 2018, Pages 315-322, ISSN 0144-8617, https://doi.org/10.1016/j.carbpol.2018.07.023.
22. Ruben Vardanyan, Victor Hruby, Chapter 31 - Antibacterial Drugs, Editor(s): Ruben Vardanyan, Victor Hruby, Synthesis of Best-Seller Drugs, Academic Press, 2016, Pages 645-667, ISBN 9780124114920, https://doi.org/10.1016/B978-0-12-411492-0.00031-6.
23. Van Den Bulcke, A I et al. “Structural and rheological properties of methacrylamide modified gelatin hydrogels.” Biomacromolecules vol. 1,1 (2000): 31-8. doi:10.1021/bm990017d.
24. Spearman, BS, Agrawal, NK, Rubiano, A, Simmons, CS, Mobini, S, Schmidt, CE. Tunable methacrylated hyaluronic acid-based hydrogels as scaffolds for soft tissue engineering applications. J Biomed Mater Res. 2020: 108A: 279– 291. https://doi.org/10.1002/jbm.a.36814.

25. C.S. Eva Hoch, Thomas Hirth, Gunter E. M. Tovar, Kirsten Borchers, Stiff gelatin hydrogels can be photo-chemically synthesized from low viscous gelatin solutions using molecularly functionalized gelatin with a high degree of methacrylation, J Mater Sci: Mater Med, 23 (2012) 2607–2617.
26. Kimura, Kotaro et al. “Preparation and in Vitro Analysis of Human Serum Albumin Nanoparticles Loaded with Anthracycline Derivatives.” Chemical & pharmaceutical bulletin vol. 66,4 (2018): 382-390. doi:10.1248/cpb.c17-00838.
27. Gao, X., Cui, Y., Levenson, R. et al. In vivo cancer targeting and imaging with semiconductor quantum dots. Nat Biotechnol 22, 969–976 (2004). https://doi.org/10.1038/nbt994.
28. Clayton, Katherine N et al. “Physical characterization of nanoparticle size and surface modification using particle scattering diffusometry.” Biomicrofluidics vol. 10,5 054107. 21 Sep. 2016, doi:10.1063/1.4962992.
29. Anita Saxena, Kumar Sachin, H.B. Bohidar, Anita Kamra Verma, Effect of molecular weight heterogeneity on drug encapsulation efficiency of gelatin nano-particles, Colloids and Surfaces B: Biointerfaces, Volume 45, Issue 1, 2005, Pages 42-48, ISSN 0927-7765, https://doi.org/10.1016/j.colsurfb.2005.07.005.
30. Khonkarn, Ruttiros et al. “PEG-OCL micelles for quercetin solubilization and inhibition of cancer cell growth.” European journal of pharmaceutics and biopharmaceutics: official journal of Arbeitsgemeinschaft fur Pharmazeutische Verfahrenstechnik e.V vol. 79,2 (2011): 268-75. doi:10.1016/j.ejpb.2011.04.011
31. Bradley L. Nilsson et al. “Electrostatic interactions regulate the release of small molecules from supramolecular hydrogels”, J. Mater. Chem. B, 2020, 8, 6366.

32. Annabi, Nasim et al. “Engineering a highly elastic human protein-based sealant for surgical applications.” Science translational medicine vol. 9,410 (2017): eaai7466. doi:10.1126/scitranslmed.aai7466.
33. Jaiswal, N et al. “Osteogenic differentiation of purified, culture-expanded human mesenchymal stem cells in vitro.” Journal of cellular biochemistry vol. 64,2 (1997): 295-312.
34. K. J. Geh, M. Hubert and G. Winter, Optimisation of one-step desolvation and scale-up of gelatine nanoparticle production, J. Microencapsulation, 2016, 33(7), 595– 604.
35. Patel, Vishal R, and Y K Agrawal. “Nanosuspension: An approach to enhance solubility of drugs.” Journal of advanced pharmaceutical technology & research vol. 2,2 (2011): 81-7. doi:10.4103/2231-4040.82950.
36. Albanese, Alexandre et al. “The effect of nanoparticle size, shape, and surface chemistry on biological systems.” Annual review of biomedical engineering vol. 14 (2012): 1-16. doi:10.1146/annurev-bioeng-071811-150124
37. Niknejad, Hassan, and Raziyeh Mahmoudzadeh. “Comparison of Different Crosslinking Methods for Preparation of Docetaxel-loaded Albumin Nanoparticles.” Iranian journal of pharmaceutical research : IJPR vol. 14,2 (2015): 385-94.
38. Anitha Ethirajan, Katrin Schoeller, Anna Musyanovych, Ulrich Ziener, and Katharina Landfester, “Synthesis and Optimization of Gelatin Nanoparticles Using the Miniemulsion Process”, Biomacromolecules 2008 9 (9), 2383-2389 doi: 10.1021/bm800377w.
39. Sun, Mingyue et al. “Synthesis and Properties of Gelatin Methacryloyl (GelMA) Hydrogels and Their Recent Applications in Load-Bearing Tissue.” Polymers vol. 10,11 1290. 21 Nov. 2018, doi:10.3390/polym10111290.

40. Snyder, R W, and D B Glasser. “Antibiotic therapy for ocular infection.” The Western journal of medicine vol. 161,6 (1994): 579-84.
41. Yoon, Hee Jeong et al. “Cold Water Fish Gelatin Methacryloyl Hydrogel for Tissue Engineering Application.” PloS one vol. 11,10 e0163902. 10 Oct. 2016, doi:10.1371/journal.pone.0163902.
42. Campbell, P. et al. “Evaluation of Absorbable Surgical Sealants: In vitro Testing.” (2005).
43. Shirzaei Sani, Ehsan et al. “Sutureless repair of corneal injuries using naturally derived bioadhesive hydrogels.” Science advances vol. 5,3 eaav1281. 20 Mar. 2019, doi:10.1126/sciadv.aav128.
44. Wang, Yihu et al. “Development of a Photo-Crosslinking, Biodegradable GelMA/PEGDA Hydrogel for Guided Bone Regeneration Materials.” Materials (Basel, Switzerland) vol. 11,8 1345. 3 Aug. 2018, doi:10.3390/ma11081345.
45. Balfour, J A, and H M Lamb. “Moxifloxacin: a review of its clinical potential in the management of community-acquired respiratory tract infections.” Drugs vol. 59,1 (2000): 115-39. doi:10.2165/00003495-200059010-00010.
46. Niels Høiby, Kaj-Åge Henneberg, Hengshuang Wang, Camilla Stavnsbjerg, Thomas Bjarnsholt, Oana Ciofu, Ulla Rydal Johansen, Thomas Sams, Formation of Pseudomonas aeruginosa inhibition zone during tobramycin disk diffusion is due to transition from planktonic to biofilm mode of growth, International Journal of Antimicrobial Agents, Volume 53, Issue 5, 2019, Pages 564-573, ISSN 0924-8579, https://doi.org/10.1016/j.ijantimicag.2018.12.015.